Synergistic Effect of Graphene Oxide/MWCNT Films in Laser Desorption/Ionization Mass Spectrometry of Small Molecules and Tissue Imaging

Young-Kwan Kim,[†] Hee-Kyung Na,[†] Sul-Jin Kwack,[†] Soo-Ryoon Ryoo,[†] Youngmi Lee,[‡] Seunghee Hong,[†] Sungwoo Hong,[†] Yong Jeong,[‡] and Dal-Hee Min[†,*]

[†]Department of Chemistry, Institute for the BioCentury, and [‡]Department of Bio and Brain Engineering, Korea Advanced Institute of Science and Technology (KAIST), 373-1 Guseong Dong, Yuseong-gu, Daejeon 305-701, Korea

ABSTRACT Matrix-assisted laser desorption/ionization mass spectrometry has been considered an important tool for various biochemical analyses and proteomics research. Although addition of conventional matrix efficiently supports laser desorption/ionization of analytes with minimal fragmentation, it often results in high background interference and misinterpretation of the spatial distribution of biomolecules especially in low-mass regions. Here, we show design, systematic characterization, and application of graphene oxide/multiwalled carbon nanotube-based films fabricated on solid substrates as a new matrix-free laser desorption/ionization platform. We demonstrate that the graphene oxide/multiwalled carbon nanotube double layer provides many advantages as a laser desorption/ionization substrate, such as efficient desorption/ionization of analytes with minimum fragmentation, high salt tolerance, no sweet-spots for mass signal, excellent durability against mechanical and photoagitation and prolonged exposure to ambient conditions, and applicability to tissue imaging mass spectrometry. This platform will be widely used as an important tool for mass spectrometry-based biochemical analyses because of its outstanding performance, long-term stability, and cost effectiveness.

KEYWORDS: carbon nanotube · graphene · mass spectrometry · nanohybrid · surface modification

Matrix-assisted desorption/ionization mass spectrometry (MALDI-MS) has become a powerful tool for biochemical analyses and proteomics research since its debut by Karas and Hillenkamp in the 1980s.[1] Soft ionization of analytes with minimum fragmentation provides mass spectra that are easy to interpret because they present intact molecular ion peaks of biomolecules.[2] Although MALDI-MS has been successful in analyzing molecules with various molecular weights from 1 to 100 kDa, the use of organic matrix molecules has resulted in several problems such as interference in the low-mass region (m/z < 500),[3] hot-spot formation by heterogeneous cocrystallization with analytes,[4] and much trial-and-error to find the appropriate matrix composition for successful analysis.[5] Thus, there have been efforts to develop a matrix-free laser desorption/ionization mass spectrometry (LDI-MS) platform, such as nanomaterial-assisted laser desorption/ionization (NALDI) and desorption/ionization on porous silicon (DIOS), for mass spectrometric analysis using inorganic nanoparticles[6−8] and porous silicon substrates,[9] which transfer absorbed energy from the laser to the analytes for ionization.

Among various nanomaterials, carbon-based nanomaterials, such as fullerene,[10,11] carbon nanotube,[12−14] and graphite,[15−17] have been actively investigated for use in LDI-MS. Recently, graphene, a single-layered graphite composed of a perfect honeycomb crystal lattice, has shown great potential for applications in LDI-MS, in addition to applications in nanoelectronic devices, transparent electrodes, and biosensors.[18−20] In addition to high LDI efficiency, the surfaces of carbon nanomaterials can be easily oxidized to present oxygen functional groups for solubilization in aqueous solvents and proton donation[14] and harnessed for enrichment of small amounts of hydrophobic molecules[21] and biomolecules.[19,22,23]

However, NALDI-MS has not been widely used due to high costs, cumbersome sample preparation, difficulty in maintaining the quality and stability of the nanomaterials, contamination of the mass spectrometer, and saturation of the detector by flight of nanomaterial itself.[24] Thus, the development of a matrix-free LDI platform that is compatible with a chip format is a prerequisite for the efficient mass spectrometric detection of small molecules. Additionally, a chip format for mass spectrometry is compatible with a high-throughput assay

* Address correspondence to dalheemin@kaist.ac.kr.

Received for review January 20, 2011 and accepted May 3, 2011.

Published online May 03, 2011
10.1021/nn200245v

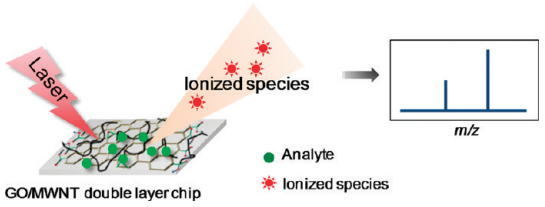

Scheme 1. Scheme of LDI-MS based on GO/MWCNT double-layer film-coated substrate.

strategy without labels or an organic matrix. In this regard, DIOS is one of the most attractive platforms that is compatible with a biochip format with proper surface chemistry, but it also requires relatively high cost and complicated fabrication process for the preparation of porous silicon.[9,25,26]

MALDI imaging mass spectrometry (IMS) is another emerging tool in various research fields, such as proteomics, lipidomics, and pharmacology, to investigate the spatial distribution of diverse biomolecules within a tissue section. In comparison with existing techniques, IMS has several notable features, such as accurate measurement of multiple biomolecules based solely on molecular weights and post-translational modification and location of specific analytes in tissue sections.[27,28] Important challenges for MALDI-IMS are the homogeneous spreading of the matrix on the tissue surface and preventing sublimation of the matrix under high vacuum during prolonged IMS experiments.[29,30] Thus, the development of a LDI platform that is compatible with a chip format would be a breakthrough in addressing these challenges in small molecule analyses and tissue imaging with mass spectrometry.

Here, a graphene oxide (GO) and aminated multiwalled carbon nanotube (MWCNT) double-layer-based LDI platform was developed for the detection of small molecules and mass spectrometric tissue imaging (Scheme 1). Because of their oppositely charged surfaces, the GO and aminated MWCNT (MWCNT-NH_2) can be immobilized as a stable double-layered structure in sequence on a solid substrate. The addition of MWCNT-NH_2 to the GO-coated surface is expected to enhance surface roughness and the surface area for analyte adsorption and, thus, increase LDI efficiency. The GO/MWCNT-NH_2 double layers would have good wettability in water due to their charged surface, absorb UV light, and efficiently convert the absorbed energy into thermal energy, as expected from the properties of GO and MWCNT-NH_2 in the solution phase.[12,31] These characteristic properties make GO/MWCNT-NH_2 double layer a promising candidate for a chip format LDI platform.

RESULTS AND DISCUSSION

The GO and MWCNT-NH_2 were prepared according to previously reported methods (Figure S1 in the Supporting Information).[32,33] Double-layer films of GO and MWCNT-NH_2 were then prepared on glass coverslips according to a previously reported method by self-assembling GO onto aminated glass coverslip and subsequent immobilization of MWCNT-NH_2.[33] Aqueous solutions of various small molecules (1 nmol/μL) including cellobiose, Leu-enkephalin, glucose, lysine, D-mannitol, and phenylalanine were then prepared, and 1 nmol of each small molecule was deposited on the GO/MWCNT-NH_2 double-layer films. After drying the sample spots under ambient conditions, the substrates were subjected to LDI-MS. Very clean mass spectra with low background signals were obtained in positive ionization mode, showing mass peaks corresponding to protonated ions, sodium, and/or potassium adducts of the analyte small molecules (cellobiose, *m/z* 365 $[M + Na]^+$; Leu-enkephalin, *m/z* 576 $[M + Na]^+$ and *m/z* 592 $[M + K]^+$; glucose, *m/z* 203 $[M + Na]^+$ and *m/z* 219 $[M + K]^+$; lysine, *m/z* 147 $[M + H]^+$, *m/z* 169 $[M + Na]^+$, and *m/z* 185 $[M + K]^+$; D-mannitol, *m/z* 205 $[M + Na]^+$ and *m/z* 221 $[M + K]^+$; phenylalanine, *m/z* 166 $[M + H]^+$, *m/z* 188 $[M + Na]^+$, and *m/z* 204 $[M + K]^+$) (Figure 1a). Metal cation adducts might be originated from residual Na^+ and K^+ which were included in the reagents used for oxidation of graphite to prepare graphene oxide (*i.e.*, potassium permanganate, sulfuric acid, and hydrogen peroxide) and/or in the analyte sample solutions as impurities. The metal cations might be strongly adsorbed on the GO surface due to the negative charge of the GO surface and difficult to remove during purification processes. Protonated species ($[M + H]^+$) would be sometimes more preferable rather than metal cation adducts especially for tandem mass analysis. In negative ion mode, clear mass spectra of glucose, mannitol, lysine, and phenylalanine were obtained which show peaks corresponding to deprotonated forms (glucose, *m/z* 179 $[M - H]^-$; mannitol, *m/z* 181 $[M - H]^-$; lysine, *m/z* 145 $[M - H]^-$; and phenylalanine, *m/z* 165 $[M - H]^-$) (Figure 1b), but no mass signal was observed with cellobiose and Leu-enkephalin. The high LDI efficiency of lysine and phenylalanine in negative ion mode could be due to the existence of a carboxylic acid group which can be easily deprotonated. It is intriguing to see that monosaccharides—glucose and mannitol—were detected, whereas disaccharide—cellobiose—was not detected in negative ion mode. The reason is not clear at this time, and further work is underway to understand the phenomena. The mass accuracy, resolution, and detection limit obtained in positive ion mode and surface density of deposited each small molecule are summarized in Figure 1c (for each mass spectrum obtained for determining limit of detection, see Figure S2 in the Supporting Information). As a control, the GO sheets dispersed in water were applied to the LDI of the small molecules. Mass spectra were obtained after depositing and drying

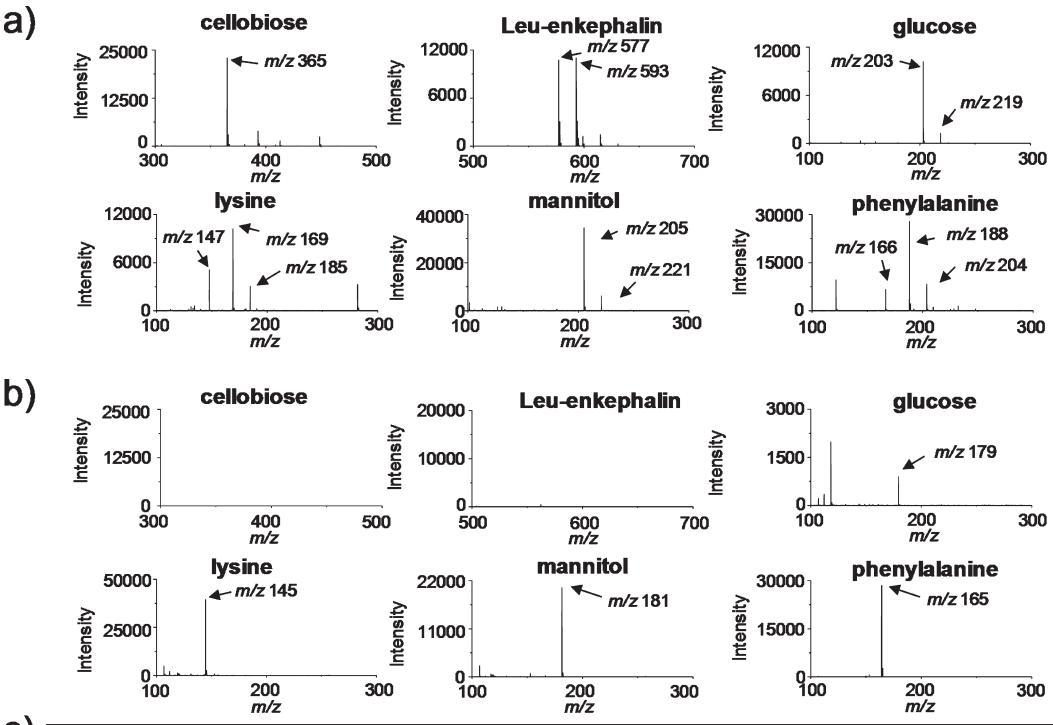

c)

Analyte	Accuracy (ppm)	Resolution	Detection limit (pmol)	Analyte spot area on GO/MWNT (mm^2)	Amount of analyte per unit area ($fmol/\mu m^2$)
Cellobiose	60	2595	10	0.3846	2.6
Leu-Enkephalin	135	3076	1	0.0314	31.0
Glucose	147	1906	10	0.3846	2.6
Lysine	59	1823	100	0.3846	2.6
Mannitol	82	1842	10	0.5024	2.0
Phenylalanine	69	2094	100	0.1256	8.0

Figure 1. Mass spectra of various small molecules obtained on GO/MWCNT-NH_2 double layer in (a) positive ion mode and (b) negative ion mode. (c) Table showing mass accuracy, resolution, detection limit, and surface density of analytes dissolved in distilled water (1 nmol/mL). Aqueous solutions of analytes were deposited on GO/MWCNT double-layer coated glass substrates and subjected to LDI-MS.

mixed solutions of the small molecules and GO in distilled water onto a stainless steel plate. Among the tested analytes, only cellobiose, phenylalanine, and enkephalin gave mass peaks with relatively high background signals in the low-mass region (m/z < 200; Figure S3a,b in the Supporting Information). This background signal might be originated from the destruction and flight of GO sheets due to intense laser irradiation. Therefore, surface immobilization of GO sheets is important to prevent high background signals.

To further investigate LDI efficiency of surface-immobilized carbon materials and to reveal which nanomaterial—GO or MWCNT-NH_2—plays a more critical role, various types of different substrates were prepared by utilizing GO, reduced GO (RGO), MWCNT, and MWCNT-NH_2. The substrates are classified into three categories—substrates coated with only GO derivatives, only MWCNT-NH_2, and combinations of GO and MWCNT derivatives (Figure 2a). GO derivative-coated chips were prepared by immobilizing GO on aminated glass substrates and by reducing the surface-immobilized GO substrates with hydrazine monohydrate solution. MWCNT-NH_2-coated substrate was prepared by immobilization of MWCNT-NH_2 onto epoxide presenting glass surface. Three different chips based on combinations of GO and MWCNT derivatives were prepared by immobilizing MWCNT onto RGO substrate (RGO/MWCNT) *via* $\pi-\pi$ interaction, adsorbing MWCNT-NH_2 onto GO substrate *via* electrostatic interaction (GO/MWCNT-NH_2), and chemical reduction of the prepared GO/MWCNT-NH_2 (RGO/MWCNT-NH_2) (Figure 2b). SEM images showed successful preparation of surface-immobilized carbon nanomaterials with high surface coverage (Figure 2c).

The LDI-MS of the small molecules was next performed on the six different carbon nanomaterial-based substrates under the same instrumental conditions (Figure S4 in the Supporting Information). The relative mass peak intensities are shown as bar graphs for comparison (Figure 3a,b). As expected, mass peak intensities were highest on the substrates where combinations of

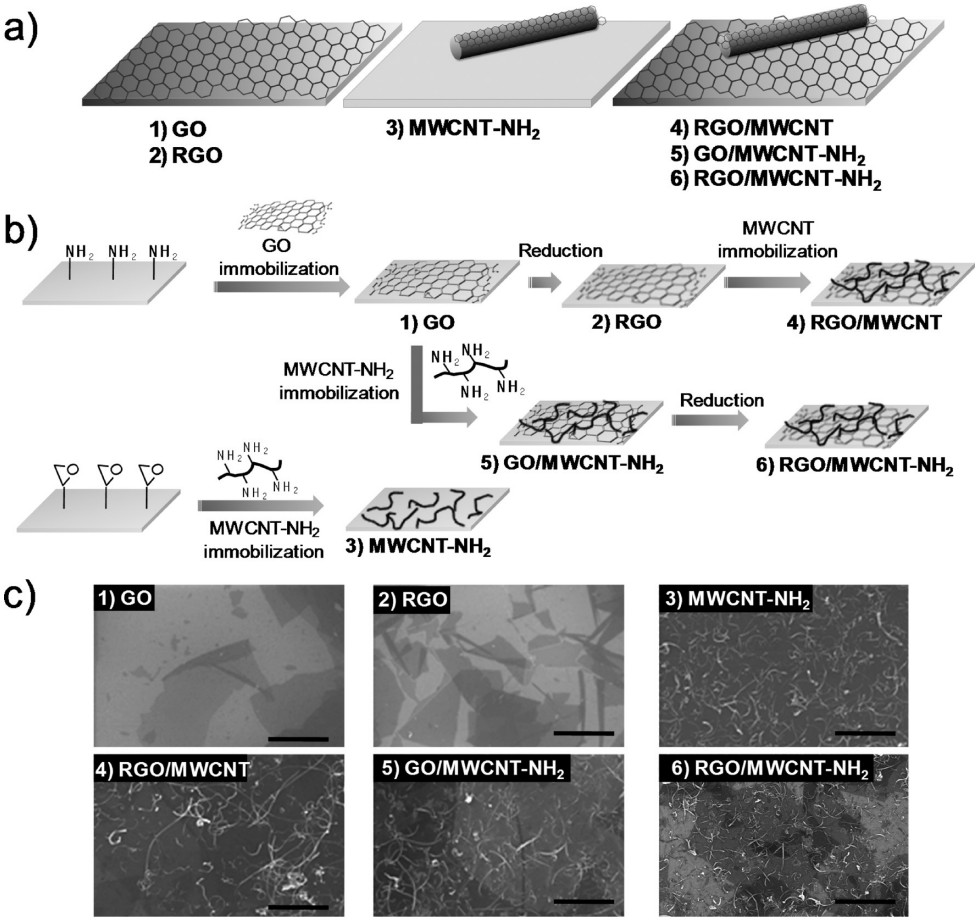

Figure 2. Various carbon nanomaterial-based substrates fabricated for comparison of LDI efficiency. (a) Scheme of three substrates composed of GO derivative-coated, MWCNT-NH_2-coated, and GO and MWCNT derivative-coated as surface immobilized films. (b) Detailed scheme of preparation of six different graphene and/or MWCNT-based substrates. (c) SEM images of the prepared carbon nanomaterial substrates. The scale bar is 1 μm.

GO and MWCNT-NH_2 were used (GO/MWCNT-NH_2 and RGO/MWCNT-NH_2). It seems that the presence of surface functional groups, such as carboxylic acids and amines, plays an important role by improving surface wettability and sample spreading. It is clear that the LDI efficiency of various small molecules was significantly improved by incorporation of MWCNT-NH_2 on the GO layer. On RGO/MWCNT-NH_2 double-layer films, the LDI efficiency of small molecules was slightly altered in comparison with their unreduced pairs. Overall, for the general purpose of small molecule analyses, GO/MWCNT-NH_2-coated surface was the best LDI substrate among the substrates we tested, whereas RGO/MWCNT-NH_2 was considered as the best substrate for hydrophobic analytes such as enkephalin and Fmoc-protected amino acids. It seems that the interactions between analytes and carbon nanomaterial chips play an important role in complicated LDI processes and some kind of synergy effect exists for efficient LDI when GO/MWCNT double layer is applied to LDI-MS. Synergy may be originated from the interface of MWCNT and GO, where analytes can receive energies from both MWCNT and GO derivatives (Figure 3c).

To investigate the relationship of the structural and surface properties of the substrates with LDI efficiency, center-line average (CLA) surface roughness and water contact angles were measured. Both GO/MWCNT-NH_2 and RGO/MWCNT-NH_2—promising LDI substrates—have relatively high CLA surface roughness among the substrates, 6.646 and 5.018 nm, respectively. In contrast, GO and RGO-coated substrates showed smooth morphology with 1.117 and 0.904 nm in CLA surface roughness. This result indicates the chemical reduction led to changes in surface morphology in addition to chemical structure. CLA surface roughness of RGO film was also slightly increased to 1.914 nm from 1.117 nm after $\pi-\pi$ interaction-induced adsorption of MWCNT (RGO/MWCNT), but the surface roughness was lower than that of RGO/MWCNT-NH_2 due to difference in the amount of surface-adsorbed MWCNTs. MWCNT film showed the highest CLA surface roughness among the prepared carbon nanomaterial chips (9.079 nm) (Figure 4a,b). On the basis of the AFM characterization, we found that efficient LDI substrates, GO/MWCNT-NH_2 and RGO/MWCNT-NH_2 double-layer films, generally showed CLA surface roughness higher

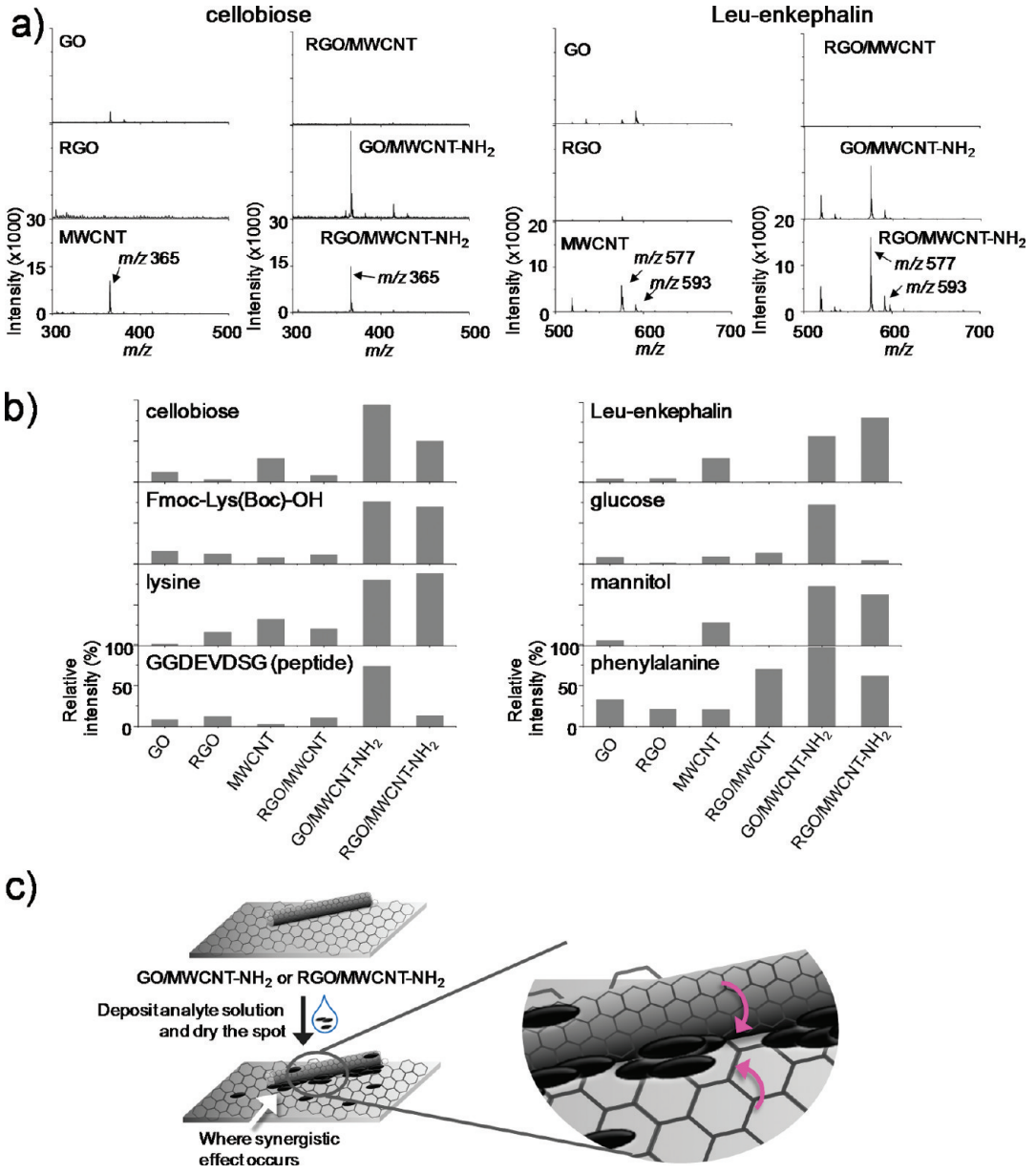

Figure 3. (a) Mass spectra of cellobiose and enkephalin (Leu-enkephalin) obtained from six different carbon nanomaterial-based films as LDI substrates. (b) Comparison of mass peak intensities of various small molecules obtained on different substrates presented as bar graphs. (c) Scheme showing synergy effect between GO and MWCNT as a LDI substrate.

than that of GO and RGO films due to adsorption of MWCNTs. Although MWCNT film showed the highest CLA surface roughness derived from the higher adsorption density of MWCNT-NH_2 than double-layered films, its LDI efficiency was inferior compared to those double-layered films. This result suggests that the GO sheets underneath MWCNTs played an important role for efficient LDI of analytes. The wettability of the substrates is also an important factor for an efficient LDI platform because it is closely related to homogeneous sample spreading. The analyte solutions were relatively well spread on GO, MWCNT, and GO/MWCNT-NH_2 films compared to the reduced ones—RGO, RGO/MWCNT, and RGO/MWCNT-NH_2 films—because of their relatively hydrophilic surfaces (Figure 4b and Figures S5 and S6 in the Supporting Information). These results well concur with the obtained water contact angle values and higher LDI efficiency of analytes on GO and GO/MWCNT-NH_2 films than on their reduced pairs.

To further investigate the complicated internal energy transfer on carbon nanomaterial films, benzylpyridinium salt (BP) was selected as a model compound to estimate survival yield—intensity of the precursor ion divided by total intensity of the fragmented and precursor ion—and desorption efficiency—absolute total intensity of the fragment and precursor ion. These values are known to be dependent on internal energy transfer processes. The low survival yield of BP on GO films, 19%, was significantly increased to 60% by

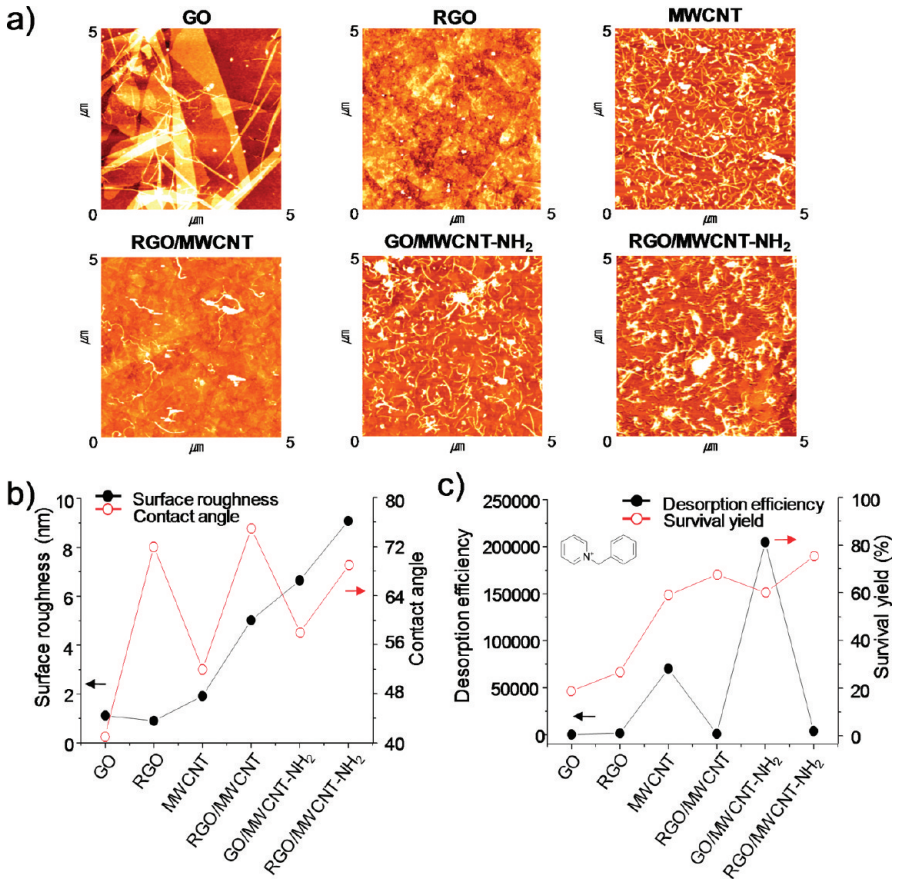

Figure 4. (a) AFM images of six different carbon nanomaterial-based films and (b) surface roughness and water contact angles of the carbon nanomaterial chips. (c) Survival yield and desorption efficiency of BP on the carbon nanomaterial chips.

incorporating MWCNT-NH_2 on GO films (GO/MWCNT-NH_2 films), and that value further increased to 27 and 76% on RGO and RGO/MWCNT-NH_2 films, respectively (Figure 4c and Figure S7 in the Supporting Information). The increased survival yields were attributed to efficient laser energy absorption and increased thermal conductivity of the GO films through incorporation of MWCNT and restoration of sp^2 carbon domains.[19] However, the desorption efficiency was considerably higher on the GO/MWCNT-NH_2 double layer than on the RGO/MWCNT-NH_2 double layer, despite its slightly lower survival yield. This low desorption efficiency on RGO/MWCNT-NH_2 may have been due to the undesired, but favorable, dissipation of absorbed laser energy into carbon material-based substrate rather than to the analytes. This energy dissipation seems more efficient in the RGO/MWCNT-NH_2 than in the GO/MWCNT-NH_2 owing to the restored sp^2 carbon domains. These results indicate that the degree of fragmentation and LDI efficiency of analytes on prepared carbon nanomaterial chips was significantly dependent on the chemical properties of the carbon nanomaterial chip and the interaction between analytes and carbon nanomaterial chips.[34]

From the series of studies, we concluded that the GO/MWCNT-NH_2 and RGO/MWCNT-NH_2 double layers were suitable for LDI of hydrophilic and hydrophobic molecules, respectively. Thus, we further characterized their advantages and performance as a novel LDI platform. Salt tolerance is an important factor of the LDI platform for the analysis of biological samples that contain high salt concentrations. To examine the salt tolerance of the GO/MWCNT-NH_2 double-layer platform, 1 μmol of small molecules tested in Figure 1 was dissolved in phosphate-buffered saline (PBS), which has an ionic strength similar to human body fluid (0.21 g/L of KH_2PO_4, 9 g/L of NaCl, and 0.72 g/L of $NaHPO_4$), spotted on the GO/MWCNT-NH_2 double layer and analyzed with LDI-ToF MS (Figure S8a,b in the Supporting Information). Although the detection limits of those small molecules were decreased by 1 order of magnitude, the GO/MWCNT-NH_2 double layer was still applicable to direct analysis of small molecules dissolved in PBS without any desalting or enrichment processes. In addition, Leu-enkephalin and phenylalanine dissolved in concentrated PBS having ion concentrations up to 1.68 g/L of KH_2PO_4, 7.20 g/L of NaCl, and 5.80 g/L of $NaHPO_4$ were successfully analyzed on the GO/MWCNT-NH_2 double layer, which confirms high salt tolerance of the GO/MWCNT-NH_2 double layer (Figure S9 in the Supporting Information). Mechanical durability is also an important factor of good

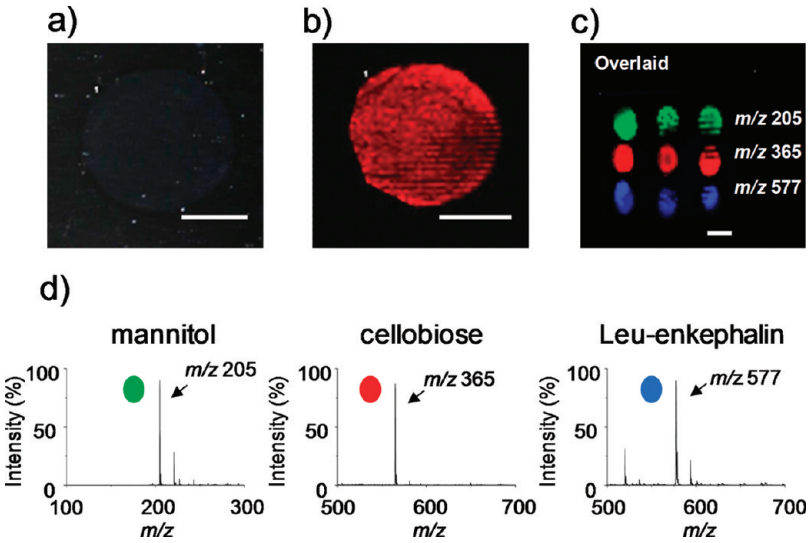

Figure 5. (a) Optical and (b) mass images of homogeneously spread cellobiose (*m/z* 365 $[M + Na]^+$) on GO/MWCNT-NH_2 substrate (scale bar = 1 mm). (c) Mass image of small molecule array composed of D-mannitol (*m/z* 205 $[M + Na]^+$), cellobiose (*m/z* 375 $[M + Na]^+$), and Leu-enkephalin (*m/z* 577 $[M + Na]^+$) along first, second, and third rows, respectively, with 1, 0.5, and 0.2 nmol formed on GO/MWCNT-NH_2 substrate (scale bar = 2 mm). (d) Mass spectra of small molecules from the spots of the array formed with 0.2 nmol of each analyte.

LDI platforms for stable, prolonged, and repeated applications for LDI-ToF MS analysis without laser irradiation-induced destruction of the nanostructures. Previously, we reported that the GO/MWCNT-NH_2 double layer had excellent mechanical durability due to the formation of covalent bonds between GO, MWCNT-NH_2, and the substrate.[33] The mechanical durability and performance as a reusable LDI substrate were successfully confirmed by repeated applications in alternating LDI-ToF MS analyses of phenylalanine and cellobiose (1 nmol each) with washing and reloading steps. Although the mass signal intensities of both small molecules gradually decreased with repeated applications in LDI-MS, the absolute intensities of the small molecules were sufficient to analyze their presence on the GO/MWCNT-NH_2 double layer even after 15 LDI analysis cycles (Figure S10a in the Supporting Information) without signs of surface destruction (Figure S10b,c in the Supporting Information) and contamination of the ionization source and the detector of mass spectrometer from GO/MWCNT-NH_2. Here, one LDI analysis cycle is defined as one complete set of procedures involving spotting and drying of analyte on the substrate, LDI-ToF MS analysis of the analyte, rinsing off the analyte by using water and ethanol, and substrate drying under a stream of nitrogen. The results show repeated applicability of GO/MWCNT-NH_2 double-layer film for LDI-MS analysis of small molecules.

Another important issue for successful LDI-ToF MS analysis is to obtain a uniform mass signal from the overall surface of the LDI-ToF MS platform without sweet-spots. To investigate spot-to-spot mass signal intensities on the GO/MWCNT-NH_2 platform, 1 μL of cellobiose solution (0.1 mM) was spotted and dried on the GO/MWCNT-NH_2 double layer, and the entire sample spot was analyzed with IMS with a raster width of 50 μm. The optical image of the GO/MWCNT-NH_2 double layer showed that homogeneous distribution of the analyte formed a circle after evaporation of the solvent, and the mass image confirmed the homogeneous distribution by showing a uniform mass signal intensity for a mass peak corresponding to cellobiose (*m/z* 365 $[M + Na]^+$; Figure 5b,e,f). As a control, 1 μL of a mixed solution of cellobiose (0.1 mM) and 2,5-dihydroxybenzoic acid (DHB) (10 mg/mL), a typical organic matrix for MALDI-ToF MS, was spotted on the glass substrate and analyzed with IMS. The mass image indicated the undesirable formation of sweet-spots due to heterogeneous crystal formation of a cellobiose-DHB (Figure S11a,b in the Supporting Information). Formation of a homogeneous sample spot with relatively uniform mass peak intensities makes the GO/MWCNT-NH_2 double-layer platform more quantitative and advantageous for monitoring chemical reactions and developing biosensors based on mass spectrometry. Moreover, the fabrication process for the GO/MWCNT-NH_2 double layer is compatible with a large-area processing and array format analysis of multiple analytes.[33] Specifically, the GO/MWCNT-NH_2 double layer was fabricated on a 2 cm^2 glass substrate, and 1 μL of each solution (1, 0.5, 0.2 mM) of D-mannitol, cellobiose, and Leu-enkephalin was spotted on the GO/MWCNT-NH_2 double layer and analyzed with IMS with a raster width of 150 μm. All of the organic molecules were successfully detected as sodium adducts from each of the array spots (3 $\times$ 3) formed on the large double-layer chip (Figure 5e,f).

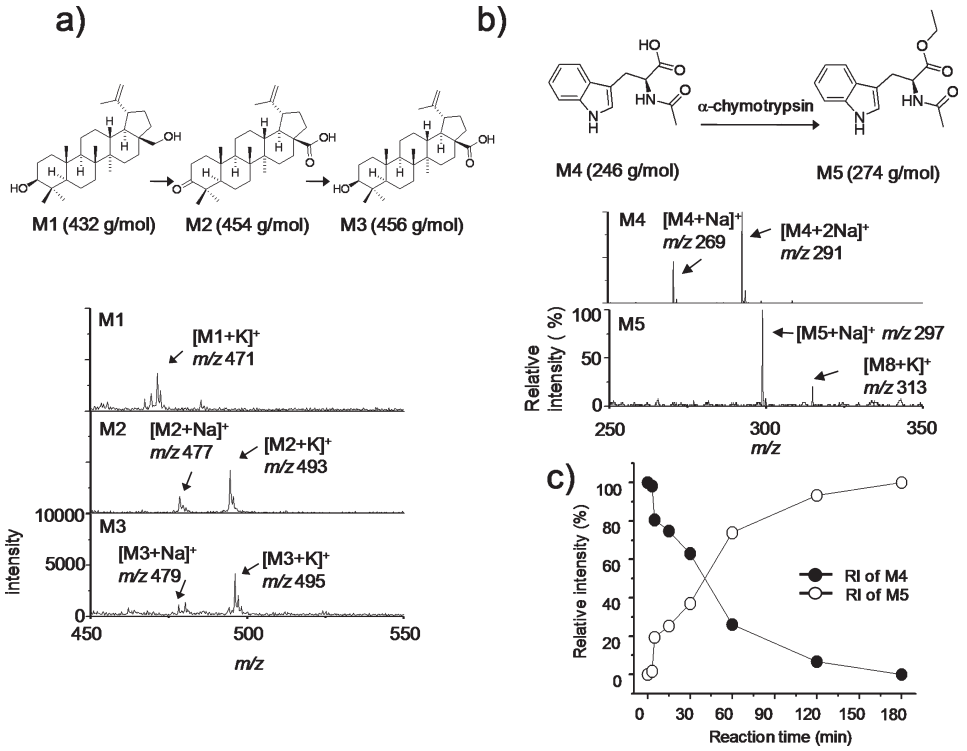

Figure 6. (a) Synthetic scheme, molecular structures of the betulin derivatives (M1, M2, M3), and mass spectra of each molecule are presented. The mass peaks corresponding to M1 ($[M1 + K]^+ = m/z$ 482), M2 ($[M2 + Na]^+ = m/z$ 477, $[M2 + K]^+ = m/z$ 493), and M3 ($[M3 + Na]^+ = m/z$ 479, $[M3 + K]^+ = m/z$ 495) were conveniently obtained on the GO/MWCNT-NH_2 double layer. (b) Molecular structures of substrates and products are shown for an enzyme-catalyzed (α-chymotrypsin) esterification. Mass spectra were obtained from the enzyme reaction mixture after 3 and 180 min of reaction time. (c) Changes in the relative mass peak intensities of M4 and M5 were plotted as a function of reaction time.

Encouraged by the excellent performance of the GO/MWCNT-NH_2 double layer as a novel LDI-ToF MS platform, we extended the application of our platform for various mass spectrometric analyses. The GO/MWCNT-NH_2 double layer was used to follow organic reactions based on changes in the molecular weight of the starting molecule to product. The conversion of the betulin (M1) starting molecule (432 g/mol) to betulinic acid (M3, 456 g/mol) by a two-step organic reaction through betulonic acid (M2, 454 g/mol) was successfully characterized on the GO/MWCNT-NH_2 double-layer LDI platform (Figure 6a). Betulin and betulinic acid have been reported to exhibit anticancer, antimalarial, anti-inflammatory, and anti-HIV activity and are widely studied anticancer agents.[35,36] The peaks corresponding to the molecules (M1, M2, M3) were not observed on stainless steel or glass substrates without the GO/MWCNT-NH_2 double layer (data not shown). As another example, conjugated cyclic organic molecules (Figure S12a in the Supporting Information) were also synthesized and analyzed with LDI-ToF MS on the GO/MWCNT double-layer platform, which gave mass peaks corresponding to each reaction product (Figure S12b in the Supporting Information). We next conducted an enzymatic synthesis of small molecules and monitored the reaction with LDI-ToF MS on the GO/MWCNT-NH_2 double-layer film. As a model reaction, the α-chymotrypsin-catalyzed synthesis of *N*-acetyl-L-tryptophan ethyl ester (M5, 274 g/mol) through esterification of *N*-acetyl-L-tryptophan (M4, 246 g/mol) was successfully characterized using the GO/MWCNT-NH_2 LDI platform with kinetic measurements (Figure 6b,c and Figure S13 in the Supporting Information).[37] Thus, the GO/MWCNT-NH_2 double-layer platform can be used to monitor chemical and biological syntheses of small organic molecules and considered as a mass spectrometry-based assay platform of enzyme activities in solution.

Finally, the RGO/MWCNT-NH_2 was applied to IMS of lipids that were distributed in mouse brain tissue. We used the RGO/MWCNT-NH_2 platform for lipid analysis, not GO/MWCNT-NH_2, because the high LDI efficiency and stronger affinity of hydrophobic molecules to the RGO/MWCNT-NH_2 double layer than to the GO/MWCNT-NH_2 double layer could be an advantage for LDI-MS of lipids.[38] The investigation of the lipid distribution and their identification are important because lipids play essential roles in biological processes, such as signal transduction, neurotransmission, myelination, apoptosis, vesicular trafficking, and transcriptional and post-translational regulation.[39] To confirm photon energy absorption on the RGO/MWCNT-NH_2 double layer and energy transfer to the tissue section, mouse

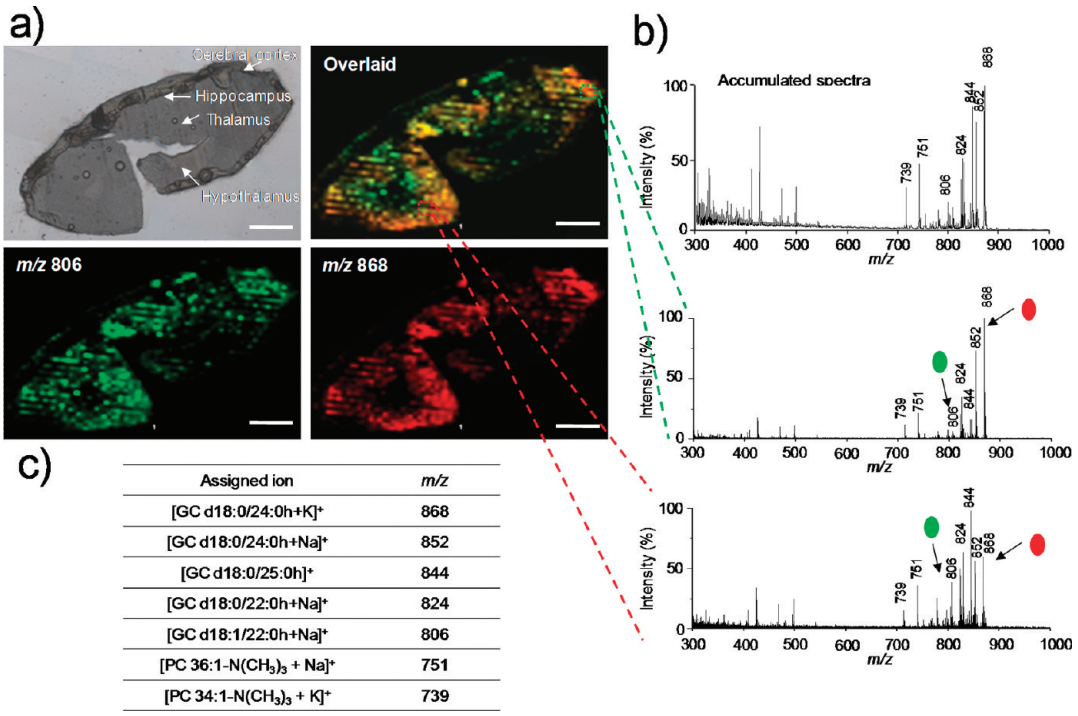

Assigned ion	*m/z*
[GC d18:0/24:0h+K]$^+$	868
[GC d18:0/24:0h+Na]$^+$	852
[GC d18:0/25:0h]$^+$	844
[GC d18:0/22:0h+Na]$^+$	824
[GC d18:1/22:0h+Na]$^+$	806
[PC 36:1-N(CH$_3$)$_3$ + Na]$^+$	751
[PC 34:1-N(CH$_3$)$_3$ + K]$^+$	739

Figure 7. (a) Optical and mass images of a mouse brain tissue slice on a RGO/MWCNT-NH$_2$ double-layer substrate. (b) Mass spectra from designated regions in the brain tissue slice in (a). (c) Summary of the species identified in the mass spectra. The mass peaks corresponding to [GC d18:0/24:0 h+K]$^+$ and [GC d18:1/22:0 h+Na]$^+$ were selected to reconstruct a total ion map.

brain tissue sections having 15 μm thickness were prepared by sagittal cutting, mounted side-by-side on the top surface of the RGO/MWCNT-NH$_2$ double layer, and analyzed with IMS with a laser beam diameter of 50 μm at the target plate and raster width of 100 μm without using any organic matrix (Figure 7a,b). All of the major ion species detected from the tissue were assigned as glycerophosphocholine (GC) and phosphatidylcholine (PC) adducts with sodium and potassium, which showed distributions in the tissue section comparable to previous reports (Figure 7c).[40,41] A total ion map was constructed using the mass peaks corresponding to [GC d18:0/24:0 h+K]$^+$ and [GC d18:1/22:0 h+Na]$^+$ (Figure 7a). Tissue slice samples required higher laser power to obtain acceptable mass spectra than small molecule samples, giving high background signals in low-mass region (*m/z* 100−300) probably due to destruction of carbon nanomaterials. Brain tissue slice of 20 μm thickness gave much lower mass peak intensities than tissue slices with 15 μm thickness on our substrate (data not shown). Therefore, for tissue analysis, possible working mass range of RGO/MWCNT-NH$_2$ double layer would be greater than *m/z* 300 with thin tissue sections having a thickness of 15 μm or smaller. The results showed that ozur RGO/MWCNT-NH$_2$ double-layer platform enables direct IMS analysis of tissue section without assistance of conventional organic matrix. Thus, we avoided disadvantages associated with organic matrix, such as difficulty in homogeneous application to the tissue surface and sublimation during the lengthy mass imaging process.

CONCLUSION

A novel LDI-MS and IMS platform was developed using GO and MWCNT as a surface-immobilized double-layer format through the self-assembly of GO sheets and aminated MWCNT on a chemically modified substrate. The fabricated GO/MWCNT-NH$_2$ and RGO/MWCNT-NH$_2$ double-layer film-coated substrates showed many advantages as a LDI-MS and IMS platform. First, the uniform mass signal intensity was obtained around the overall surface of the GO/MWCNT-NH$_2$ double-layer substrate without sweet-spots, which is an advantage for biochip applications. Second, the fabricated double-layer platform was very durable against mechanical and photoagitation, preventing the undesirable ionization source contamination and detector saturation induced by laser irradiation and allowing repeated use of the double-layer platform. Third, the double-layer platform showed an excellent salt tolerance and no fragmentation of analytes. Fourth, the LDI efficiency of the double layer remained stable even after prolonged exposure to atmospheric conditions, for up to several months. Fifth, the reduced pair of the GO/MWCNT-NH$_2$ double-layer platform was readily applicable to IMS MS. Finally, the present GO/MWCNT-NH$_2$ and RGO/MWCNT-NH$_2$ double-layer platforms are substantially more cost-effective than existing chip format LDI platforms and

meet almost all of the important demands of a LDI platform. Collectively, the present LDI substrate would be useful in a real-life analysis of body fluids and tissues by reducing interferences from high salt concentration and organic matrix which are considered as drawbacks of conventional MALDI-ToF MS. Although high laser energy might sometimes give background peaks from the destruction of the coated carbon nanomaterials, typical laser power required for obtaining mass spectra of analytes from our substrates did not give notable backgrounds under our experimental conditions. In conclusion, we expect that the present LDI platform based on graphene derivatives and MWCNT will be an important, practical, and widely useful tool in LDI-MS and IMS research fields.

METHODS

Materials. Natural graphite (FP 99.95% pure) was purchased from Graphit Kropfmühl AG (Hauzenberg, Germany). Multiwalled carbon nanotube (MWCNT), 15 nm diameter and 20 μm length, was purchased from Nanolab (USA). Sodium nitrate and hydrogen peroxide (30% in water) were purchased from Junsei (Japan). Potassium permanganate, 3-aminopropyltriethoxysilane (APTES), ethylene diamine, and anhydrous dimethylformamide (DMF) were purchased from Sigma-Aldrich (St. Louis, MO, USA). Nitric acid and sulfuric acid were purchased from Samchun (Seoul, Korea). 1-Undecanol was purchased from Tokyo Chemical Industry (Tokyo, Japan). Ethanol was purchased from Merck (Darmstadt, Germany),and 500 nm SiO_2/P^{2+} Si substrates (500 μm in thickness) and 4 in. quartz wafers (500 μm in thickness) were purchased from STC (Japan) and i-Nexus (Stamford, USA), respectively. All chemicals were used as received.

Preparation of GO and GO/MWCNT-NH_2 Double-Layer Thin Films. For the preparation of GO thin films, the APTES-functionalized glass substrate was immersed in an aqueous GO suspension (1.5 mg/mL) for 1 h, washed with water and ethanol, dried under a stream of nitrogen, and baked at 125 °C for 10 min under nitrogen flow. The GO thin-film-coated substrate was used to fabricate the GO/MWCNT-NH_2 double layer as a support. The substrate was immersed in the MWCNT-NH_2 suspension (120 μg/mL) for 1 h, washed with water and ethanol, and dried under a stream of nitrogen. The GO/MWCNT-NH_2 double-layer-coated substrate was baked at 125 °C for 10 min on a heated plate under nitrogen flow.

Preparation of the Reduced GO (RGO) and RGO/MWCNT-NH_2 Double-Layer Thin Films. The GO and GO/MWCNT-NH_2 double-layer thin-film-coated substrates were immersed in a 20% hydrazine monohydrate solution in DMF for a day at 80 °C, washed with DMF, water, and ethanol, and dried under a stream of nitrogen. The reduced GO and GO/MWCNT-NH_2 double-layer thin-film-coated substrates were used as counter pairs to study the influence of the chemical structure of carbon nanomaterials on the LDI efficiency of small molecules.

Preparation of the RGO/MWCNT Double Layer Using a MWCNT Suspension. MWCNTs (10 mg) were dispersed in 10 mL of dichlorobenzene by sonication for 1 h and centrifuged (3099 rcf, 10 min) to remove large aggregates of MWCNTs. The RGO thin-film-coated substrate was immersed in the MWCNT suspension for 1 h, washed with water and ethanol, and dried under a stream of nitrogen.

Preparation of MWCNT-NH_2-Coated Glass Substrates. The piranha-treated glass substrate was immersed in a 10 mM anhydrous toluene solution of 3-glycidylpropyltriethoxysilane for 30 min, washed with ethanol and water, and dried under a stream of nitrogen. The substrate was immersed in a 120 μg/mL of MWCNT-NH_2 suspension for 1 h, washed with water and ethanol, and dried under a stream of nitrogen. The MWCNT-NH_2-coated substrate was baked at 125 °C for 15 min on a heated plate under nitrogen flow.

Analysis of Organic Molecules. The various analytes, including sugars, peptides, amino acids, and protected amino acids, were dissolved in water at 1 nmol/μL. Aliquots of 1 μL of the prepared solutions were spotted on the carbon nanomaterial chips, allowed to dry under ambient conditions, inserted into the MALDI-ToF MS, and analyzed under the same experimental conditions. This sample preparation protocol was applied to all of the small organic molecule analyses, including IMS, on the RGO/MWCNT double-layer platform.

Reusability Test of GO/MWCNT-NH_2 Double-Layer Thin Film. One microliter of 1 mM (1 nmol) cellobiose and phenylalanine solutions was spotted on the GO/MWCNT-NH_2 double layer, allowed to dry under ambient conditions, inserted into the MALDI-ToF MS, and analyzed under the same experimental conditions. After analysis, the GO/MWCNT-NH_2 double layer was thoroughly washed with water and ethanol and dried under a stream of nitrogen. The cleaned GO/MWCNT-NH_2 double layer was repeatedly applied to analysis of cellobiose and phenylalanine. Above processes were repeated up to 15 cycles.

Enzyme-Catalyzed Synthesis. *N*-Acetyl-L-tryptophan (1.2 mg) and 29 μL of ethanol were dissolved in 500 μL of chloroform and mixed with 100 μL of an α-chymotrypsin solution (10 mg/mL). The mixture was shaken on a horizontal shaker at 600 rpm for 3 h. An aliquot of 1 μL of the chloroform phase was spotted on the GO/MWCNT-NH_2 double layer at 3, 5, 15, 30, 60, 120, and 180 min.

Preparation of the Mouse Brain Tissue Section. After anesthetizing by i.p. injection of a mixture of ketamine and xylazine (4:1, 0.005 mg/g body weight), the mice (C57/BL6) were decapitated. After removing the skull, the brain was isolated and immersed in liquid nitrogen for about 5 min. After the brain was frozen, brain slices were prepared with a thickness of 15 μm in the coronal direction at −25 °C using a cryotome (CM 1850, Leica, Nusslach, Germany) and immediately mounted on the RGO/MWCNT-NH_2 double layer platform.

Characterization. The morphology of the carbon nanomaterial chips was observed by S-4800 field emission scanning electron microscopy (Hitachi, Japan). All AFM images and profiles of carbon nanomaterials were obtained with an XE-100 (Park System, Korea) with a backside gold-coated silicon SPM probe (M to N, Korea). All mass spectrometric analyses were carried out by using a Bruker Autoflex III (Bruker Daltonics, Germany) equipped with a Smartbeam laser (Nd:YAG, 355 nm, 100 Hz, 50 μm in spot diameter at target plate) in positive and negative reflective modes. The accelerating voltage was 19 kV, and all spectra were obtained by averaging 500 laser shots unless otherwise indicated. Raman characterization was performed by LabRAM HR UV/vis/NIR (Horiba Jobin Yvon, France) using an Ar ion CW laser (514.5 nm) as an excitation source focused through a BXFM confocal microscope equipped with an objective (50×, numerical aperture = 0.50). The UV−vis spectra were recorded with a UV-2550 (Shimadzu, Japan). FT-IR spectra measurements of graphite oxide were performed with an EQUINOX55 (Bruker, Germany) using the KBr pellet method.

Acknowledgment. This work was supported by the Basic Science Research Program through the National Research Foundation of Korea (NRF), funded by the Korean government (MEST) (Grant Nos. 313-2008-2-C00538, R01-2008-000-20301-0, 2010-0015340, 2010-0022179, 2011-0017356), and by the Nano R&D program of NRF funded by MEST (2008-2004457).

Supporting Information Available: Analytical data. This material is available free of charge *via* the Internet at http://pubs.acs.org.

REFERENCES AND NOTES

1. Karas, M.; Bachman, D.; Bahr, U.; Hillenkamp, F. Matrix-Assisted Ultraviolet Laser Desorption of Non-volatile Compounds. *Int. J. Mass Spectrom. Ion Process* **1987**, *78*, 53–68.
2. Karas, M.; Hillenkamp, F. Laser Desorption Ionization of Proteins with Molecular Masses Exceeding 10000 Da. *Anal. Chem.* **1988**, *60*, 2299–2301.
3. Guo, Z.; Zhang, Q.; Zou, H.; Guo, B.; Ni, J. A Method for the Analysis of Low-Mass Molecules by MALDI-TOF Mass Spectrometry. *Anal. Chem.* **2002**, *74*, 1637–1641.
4. Tholey, A.; Heinzle, E. Ionic (Lliquid) Matrices for Matrix-Assisted Laser Desorption/Ionization Mass Spectrometry: Applications and Perspectives. *Anal. Bioanal. Chem.* **2006**, *386*, 24–37.
5. Kawasaki, H.; Sugitani, T.; Watanabe, T.; Yonezawa, T.; Moriwaki, H.; Arakawa, R. Layer-by-Layer Self-Assembled Mutilayer Films of Gold Nanoparticles for Surface-Assisted Laser Desorption/Ionization Mass Spectrometry. *Anal. Chem.* **2008**, *80*, 7524–7533.
6. Tanaka, K.; Waki, H.; Ido, Y.; Akita, S.; Yoshida, Y.; Yoshida, T.; Matsuo, T. Protein and Polymer Analyses up to *m/z* 100,000 by Laser Ionization Time-of-Flight Mass Spectrometry. *Rapid Commun. Mass Spectrom.* **1988**, *2*, 151–153.
7. Kinumi, T.; Saisu, T.; Takayama, M.; Niwa, H. Matrix-Assisted Laser Desorption/Ionization Time-of-Flight Mass Spectrometry Using an Inorganic Particle Matrix for Small Molecule Analysis. *J. Mass Spectrom.* **2000**, *35*, 417–422.
8. Mclean, J. A.; Stumpo, K. A.; Russell, D. H. Size-Selected (2−10 nm) Gold Nanoparticles for Matrix Assisted Laser Desorption Ionization of Peptides. *J. Am. Chem. Soc.* **2005**, *127*, 5304–5305.
9. Wei, J.; Buriak, J. M.; Siuzdak, G. Desorption−Ionization Mass Spectrometry on Porous Silicon. *Nature* **1999**, *399*, 243–246.
10. Hopwood, F. G.; Michalak, L.; Alderdice, D. S.; Fisher, K. J.; Willet, G. D. C60-Assisted Laser Desorption/Ionization Mass Spectrometry in the Analysis of Phosphotungstic Acid. *Rapid Commun. Mass Spectrom.* **1994**, *8*, 881–885.
11. Shiea, J.; Huang, J. P.; Teng, C. F.; Jeng, J.; Wang, L. Y.; Chiang, L. Y. Use of Water-Soluble Fullerene Derivative as Precipitating Reagent and Matrix Assisted Laser Desorption/Ionization Matrix To Selectively Detect Charged Species in Aqueous Solutions. *Anal. Chem.* **2003**, *75*, 3587–3595.
12. Xu, S.; Li, Y.; Zou, H.; Qiu, J.; Guo, Z.; Guo, B. Carbon Nanotubes as Assisted Matrix for Laser Desorption/Ionization Time-of-Flight Mass Spectrometry. *Anal. Chem.* **2003**, *75*, 6191–6195.
13. Ugarov, M. V.; Egan, T.; Khabashesku, D. V.; Schultz, J. A.; Peng, H.; Khabashesku, V. N.; Furutani, H.; Prather, K. S.; Wang, H. W.; Jackson, S. N.; *et al.* MALDI Matrices for Biomolecular Analysis Based on Functionalized Carbon Nanomaterials. *Anal. Chem.* **2004**, *76*, 6734–6742.
14. Ren, S. F.; Guo, Y. L. Oxidized Carbon Nanotubes as Matrix for Matrix-Assisted Laser Desorption/Ionization Time-of-Flight Mass Spectrometric Analysis of Biomolecules. *Rapid Commun. Mass Spectrom.* **2005**, *19*, 255–260.
15. Sunner, J.; Dratz, E.; Chen, Y. C. Graphite Surface-Assisted Laser Desorption/Ionization Time-of-Flight Mass Spectrometry of Peptides and Proteins from Liquid Solutions. *Anal. Chem.* **1995**, *67*, 4335–4342.
16. Dale, D. J.; Knochenmuss, R.; Zenobi, R. Graphite/Liquid Mixed Matrixes for Laser Desorption/Ionization Mass Spectrometry. *Anal. Chem.* **1996**, *68*, 3321–3329.
17. Zhang, H.; Cha, S.; Yeung, E. S. Colloidal Graphite-Assisted Laser Desorption/Ionization MS and MSn of Small Molecules. 2. Direct Profiling and MS Imaging of Small Metabolites from Fruits. *Anal. Chem.* **2007**, *79*, 6575–6584.
18. Dong, X.; Cheng, J.; Li, J.; Wang, Y. Graphene as a Novel Matrix for the Analysis of Small Molecules by MALDI-TOF MS. *Anal. Chem.* **2010**, *82*, 6208–6214.
19. Tang, L. A.; Wang, J.; Loh, K. P. Graphene-Based SELDI Probe with Ultrahigh Extraction and Sensitivity for DNA Oligomer. *J. Am. Chem. Soc.* **2010**, *132*, 10976–10977.
20. Zhou, X.; Wei, Y.; He, Q.; Boey, F.; Zhang, Q.; Zhang, H. Reduced Graphene Oxide Films Used as Matrix of MALDI-TOF-MS for Detection of Octachlorodibenzo-*p*-dioxin. *Chem. Commun.* **2010**, *46*, 6974–6976.
21. Pan, C.; Xu, S.; Zou, H.; Guo, Z.; Zhang, Y.; Guo, B. Carbon Nanotubes as Adsorbent of Solid-Phase Extraction and Matrix for Laser Desorption/Ionization Mass Spectrometry. *J. Am. Soc. Mass Spectrom.* **2005**, *16*, 263–270.
22. Hen, W. Y.; Wang, L. S.; Chiu, H. T.; Chen, Y. C.; Lee, C. Y. Carbon Nanotubes as Affinity Probes for Peptides and Proteins in MALDI MS Analysis. *J. Am. Soc. Mass Spectrom.* **2004**, *15*, 629–635.
23. Larsen, M. R.; Cordwell, S. J.; Roepstorff, P. Graphite Powder as an Alternative or Supplement to Reversed-Phase Material for Desalting and Concentration of Peptide Mixtures Prior to Matrix-Assisted Laser Desorption/Ionization-Mass Spectrometry. *Proteomics* **2002**, *2*, 1277–1287.
24. Han, M.; Sunner, J. An Activated Carbon Substrate Surface for Laser Desorption Mass Spectrometry. *J. Am. Soc. Mass Spectrom.* **2000**, *11*, 644–649.
25. Thomas, J. J.; Shen, Z.; Crowell, J. E.; Finn, M. G.; Siuzdak, G. Desorption/Ionization on Silicon (DIOS): A Diverse Mass Spectrometry Platform for Protein Characterization. *Proc. Natl. Acad. Sci. U.S.A.* **2001**, *98*, 4932–4937.
26. Lewis, W.; Shen, Z.; Finn, M. G.; Siuzdak, G. Desorption/Ionization on Silicon (DIOS) Mass Spectrometry: Background and Applications. *Int. J. Mass Spectrom.* **2003**, *226*, 107–116.
27. Cornett, D. S.; Reyzer, M. L.; Chaurand, P.; Caprioli, R. M. MALDI Imaging Mass Spectrometry: Molecular Snapshots of Biochemical Systems. *Nat. Methods* **2007**, *4*, 828–833.
28. Schwamborn, K.; Caprioli, R. M. Molecular Imaging by Mass Spectrometry: Looking beyond Classical Histology. *Nat. Rev. Cancer* **2010**, *10*, 639–646.
29. Leinweber, B. D.; Tsaprailis, G.; Monks, T. J.; Lau, S. S. Improved MALDI-TOF Imaging Yields Increased Protein Signals at High Molecular Mass. *J. Am. Soc. Mass Spectrom.* **2009**, *20*, 89–95.
30. Yanes, O.; Woo, H. K.; Northen, T. R.; Oppenheimer, S. R.; Shriver, L.; Apon, J.; Estrada, M. N.; Potchoiba, M. J.; Steenwyk, R.; Manchester, M.; *et al.* Nanostructure Initiator Mass Spectrometry: Tissue Imaging and Direct Biofluid Analysis. *Anal. Chem.* **2009**, *81*, 2969–2975.
31. Zhou, Y.; Bao, Q.; Varghese, B.; Tang, L. A.; Tan, C. K.; Sow, C. H.; Loh, K. P. Microstructuring of Graphene Oxide Nanosheets Using Direct Laser Writing. *Adv. Mater.* **2010**, *22*, 67–71.
32. Hummers, W. S.; Offeman, R. E. Preparation of Graphitic Oxide. *J. Am. Chem. Soc.* **1958**, *80*, 1339.
33. The detailed mechanism of GO/MWCNT-NH_2 double layer formation and its characterization have been previously reported. For more information, see: Kim, Y.-K.; Min, D.-H. Durable Large-Area Thin Films of Graphene/Carbon nanotube Double Layers as a Transparent Electrode. *Langmuir* **2009**, *25*, 11302–11306.
34. Tang, H. W.; Ng, K. M.; Lu, W.; Che, C. M. Ion Desorption Efficiency and Internal Energy Transfer in Carbon-Based Surface-Assisted Laser Desorption/Ionization Mass Spectrometry: Desorption Mechanism(s) and the Design of SALDI Substrates. *Anal. Chem.* **2009**, *81*, 4720–4729.
35. Cichewicz, R. H.; Kouzi, S. A. Chemistry, Biological Activity, and Chemotherapeutic Potential of Betulinic Acid for the Prevention and Treatment of Cancer and HIV Infection. *Med. Res. Rev.* **2004**, *24*, 90–114.
36. Alakurtti, S.; Bergström, P.; Sacerdoti-Sierra, N.; Jaffe, C. L.; Yli-Kauhaluoma, J. Anti-Leishmanial Activity of Betulin Derivatives. *J. Antibiot.* **2010**, *63*, 123–126.
37. Klibanov, A.; Samokhin, G. P.; Martinek, K.; Berezin, I. V. A New Approach to Preparative Enzymatic Synthesis. *Biotechnol. Bioeng.* **1977**, *19*, 1351–1361.
38. Our group previously reported lipid LDI MS on GO/MWCNT-NH_2 substrate. After the publication, we discovered that RGO/MWCNT-NH_2 substrate is a slightly better platform than GO/MWCNT-NH_2 for lipid analysis. For

details, see: Lee, J.; Kim, Y. -K.; Min, D.-H. Laser Desorption/Ionization Mass Spectrometric Assay for Phospholipase Activity Based on Graphene Oxide/Carbon Nanotube Double-Layer Films. *J. Am. Chem. Soc.* **2010**, *132*, 14714–14717.
39. van Meer, G.; Voelker, D. R.; Feigenson, G. W. Membrane Lipids: Where They Are and How They Behave. *Nat. Rev. Mol. Cell Biol.* **2008**, *9*, 112–124.
40. Cha, S.; Yeung, E. S. Colloidal Graphite-Assisted Laser Desorption/Ionization Mass Spectrometry and MSn of Small Molecules. 1. Imaging of Cerebrosides Directly from Rat Brain Tissue. *Anal. Chem.* **2007**, *79*, 2373–2385.
41. Astigarraga, E.; Barreda-Gómez, G.; Lombardero, L.; Fresnedo, O.; Castaño, F.; Giralt, M. T.; Ochoa, B.; Rodríguez-Puertas, R.; Fernández, J. A. Profiling and Imaging of Lipids on Brain and Liver Tissue by Matrix-Assisted Laser Desorption/Ionization Mass Spectrometry Using 2-Mercaptobenzothiazole as a Matrix. *Anal. Chem.* **2008**, *80*, 9105–9114.